energies

MDPI

Article

A Solution to the Problem of Electrical Load Shedding Using Hybrid PV/Battery/Grid-Connected System: The Case of Households' Energy Supply of the Northern Part of Cameroon

Ruben Zieba Falama [1,2,*], Felix Ngangoum Welaji [2], Abdouramani Dadjé [3], Virgil Dumbrava [4,*], Noël Djongyang [5], Chokri Ben Salah [6] and Serge Yamigno Doka [7]

1 Faculty of Mines and Petroleum Industries, University of Maroua, Maroua P.O. Box 46, Cameroon
2 Laboratory of Energy Research, Institute for Geological and Mining Research, Yaoundé P.O. Box 4110, Cameroon; nglix@live.fr
3 School of Geology and Mining Engineering, University of Ngaoundéré, Ngaoundéré P.O. Box 454, Cameroon; abdouramanid@gmail.com
4 Department of Power Systems, Faculty of Power Engineering, University POLITEHNICA of Bucharest, Splaiul Independentei, no 313, District 6, 060042 Bucharest, Romania
5 Department of Renewable Energy, National Advanced Polytechnic School, University of Maroua, Maroua P.O. Box 46, Cameroon; noeldjongyangl@gmail.com
6 LASEE Laboratory, ISSAT of Sousse, Department of Electrical Engineering, University of Sousse, ENIM, Monastir, Tunisia; chokribs@yahoo.fr
7 Faculty of Sciences, University of Ngaoundéré, Ngaoundéré P.O. Box 454, Cameroon; numami@gmail.com
* Correspondence: rubenziebafalama@gmail.com (R.Z.F.); v_dumbrava@yahoo.com (V.D.)

Abstract: A techno-economic study of a hybrid PV/Battery/Grid-connected system for energy supply is carried out in this paper to respond to the problem of electrical load shedding. An optimal design of the system is realized thanks to a double-objective optimization based on a proposed operational strategy of the system and on Firefly Algorithm (FA). The system is designed for household energy supply in three different towns of the northern part of Cameroon. For different *LPSP* (Loss of Power Supply Probability), the double objective simulation determines the optimal configurations of the system with their related cost. The optimal and reliable PV/Battery subsystem configuration corresponding to LPSP of 0% obtained for one household is composed for the towns of Maroua and Garoua by 8 PV modules and a battery capacity of 11.304 kWh with 1-day autonomy. For the town of Ngaoundéré, it is composed by 10 PV modules and battery capacity of 11.304 kWh with 1-day autonomy. The related investment costs corresponding to these optimal configurations are USD 6225.6 for Maroua and Garoua and USD 7136.6 for Ngaoundéré. The great proportion of the monthly energy demand consumed by the load is provided by the PV/Battery system. The monthly PV/Battery energy represents 60.385% to 72.546% of the load consumed in Maroua, 58.371% to 71.855% of the load consumed in Garoua, and 61.233% to 74.160% of the load consumed in Ngaoundéré. The annual main grid energy consumed for one household is 1299.524 kWh in Maroua, 1352.818 kWh in Garoua, and 1260.876 kWh in Ngaoundéré. Moreover, the annual PV/Battery energy consumed for one household is 1580.730 kWh in Maroua, 1527.815 kWh in Garoua, and 1619.530 kWh in Ngaoundéré. Thus, the PV/Battery system, by reducing the grid energy consumption, acts as the principal source of energy of the whole system. The time the PV/Battery/Grid-connected system needs to be economically more advantageous than the electric grid without blackouts is 17 years for Maroua and 18 years for both Garoua and Ngaoundéré. It is demonstrated in this paper that the hybrid PV/Battery/Grid-connected system is an effective solution for electrical load shedding in sub-Saharan zones. This system is very useful for grid energy consumption reduction. For a long-term investment, the PV/Battery/Grid-connected system is more economically advantageous than the main grid alone.

Keywords: techno-economic study; optimal design; FA; investment cost; *LPSP*

Citation: Zieba Falama, R.; Ngangoum Welaji, F.; Dadjé, A.; Dumbrava, V.; Djongyang, N.; Salah, C.B.; Doka, S.Y. A Solution to the Problem of Electrical Load Shedding Using Hybrid PV/Battery/Grid-Connected System: The Case of Households' Energy Supply of the Northern Part of Cameroon. *Energies* **2021**, *14*, 2836. https://doi.org/10.3390/en14102836

Academic Editor: Branislav Hredzak

Received: 19 April 2021
Accepted: 11 May 2021
Published: 14 May 2021

1. Introduction

The problem of the availability of electrical energy still remains a very serious problem in developing countries. Since electricity is at the center of development, it is very difficult for these countries to take off amid this deficit. The situation is even more serious in the countries of sub-Saharan Africa, where poverty is often accentuated because of the lack of electrical energy. According to forecasts by the World Bank, 650 million people will still lack access to electricity in 2030, and nine out of 10 of those people will be in sub-Saharan Africa [1]. Electricity is involved in almost all aspects of daily life. Electricity is needed for heating, for cooking, for transport, for telecommunications, for lighting, to power machines in industries, etc. To summarize, electricity is essential for the socio-economic development of a country, and it improves the living conditions of populations.

It is true that some countries in sub-Saharan Africa have made great progress related to urban and rural electrification. However, these countries face the problem of electrical load shedding (electricity interruption) due to natural phenomena, to forecast failure, or to the aging of the facilities that have lost their performance, thus influencing electricity production. By mentioning natural phenomena as the cause of electrical load shedding, one refers to a lack of natural resources that play a determining role in the process of producing electrical energy such as water, wind, sun, etc. Failure forecasting is the lack of planning electricity production according to future needs because the population is expected to grow. If this detail is not initially taken into account, then the installed power supply system will be unable to meet the load demand after some time, resulting in network disturbances and frequent electricity interruption.

Cameroon, a country of sub-Saharan Africa, has shown significant progress concerning electrification in recent years. However, since 2020, the northern part of Cameroon has faced a real problem of electrical load shedding due to a hydrological deficit. A weekly program of daily access to electricity is broadcast on social media every weekend by the national electricity distribution company. This partial daily availability of electricity is not without consequences for the socio-economic life of this part of the country. Nighttime, with no electricity available, are favorable for thefts and assaults. Some factories are shut down or are operating part time. Keeping food in the refrigerator is no longer an absolute guarantee. Small and large-scale economic activities are often at a standstill at times when there is no electricity. Many households use a diesel generator (DG) for electricity supply at the time when the grid connection is interrupted. Note, however, that the use of DGs is very polluting.

Previous studies have been carried out to improve the availability of electrical energy in some localities facing the issues of electrical load shedding or electrical blackouts based on a proper load shedding scheduling program [2–7]. Syadly et al. [2] have proposed an improved load shedding scheduling strategy to tackle the problem of power outages occurring in the locality of Sumatra. The proposed strategy is based on the Round Robin method. They have shown in their work that a proper scheduling program could overcome the energy deficit problem. Hirodontis et al. [3] studied the load shedding in a distribution network. Based on Swing equation (for the evaluation of the magnitude of the disturbance) and on dynamic simulation using PSCAD (Power System Analysis Package), they have demonstrated the improvement of the stability and the reliability of the distribution network submitted to load shedding. Faranda et al. [4] developed a new load shedding control strategy called "distributed interruptible load shedding". This approach for load shedding programs is a powerful tool to ensure improvement of the energy supply's reliability.

Smart grids based on hybrid systems also appear as a promising concept for electrical blackout problems [8–22]. Mansour et al. [9] developed an optimal operation of hybrid PV-battery system considering grid scheduled blackouts and battery lifetime. The PV-battery system is considered to replace the grid during blackouts periods. By applying an economic model predictive control (EMPC) to optimize the operation of the system, the obtained results have shown that the proposed method leads to the reduction in the grid energy consumption, the decrease in the PV generated power, and the maximization of the

battery lifetime. Bastholm and Fiedler [10] performed a techno-economic study of a PV-diesel hybrid system connected to the national power grid of Tanzania subject to frequent blackouts. The aim of their work was to study the impact of the blackouts on the viability of the system. The obtained results based on simulation in HOMER (a software now produced by UL in USA) have demonstrated that the PV-diesel hybrid system connected to the grid with blackouts is economically more important than the grid without blackouts. Alibakhsh et al. [11] studied the feasibility of a hybrid photovoltaic/diesel/biogas to meet the energy demand of a grid-connected village located in the east of Iran. An optimal design and technical analysis of the system has been realized under different economic conditions using HOMER software. The obtained results showed that the proposed hybrid system is reliable and economically feasible at a low cost. Samy et al. [12] proposed a hybrid PV-wind-fuel cell system as a backup system to replace the grid during blackout periods in Hurghada, Egypt. An optimal economic study of the proposed system is realized using hybrid search optimization technique. Simulation results have shown that the proposed system is economically viable and more cost-effective than electricity from the grid for commercial users in Egypt. Murphy et al. [13] proposed a hybrid solar/diesel system connected to an unreliable electric grid to provide more reliable electricity in a village in Uganda. Thanks to HOMER simulation software and a developed method, the optimal system configurations and the electricity costs for reliable power generation were determined. Simulation results showed that diesel is the most economical choice for a backup system, yet hybrid solar/diesel is the most reliable backup system and could be economically competitive with diesel backup systems in the long-term. Ali Saleh Aziz et al. [14] studied the feasibility of grid-connected and islanded operation of a solar PV micro-grid system in Iraq. The analysis of the system is based on HOMER software using five different control strategies. The obtained results showed that the hybrid PV grid-connected system can provide clean, economical, and continuous electricity production in countries with daily blackouts. Adefarati and Bansal [15] studied the impacts of a PV/wind/diesel/electric storage hybrid system on the reliability of a power system. A modified Roy Billinton test system (RBTS) distribution network was used to perform this study. It was demonstrated that the proposed hybrid system could increase the reliability of the system and reduce the power outages associated with the distribution network. An optimal operation strategy of a hybrid PV-battery system under grid scheduled blackouts was performed by Mansour et al. [23]. The city of Gaza in Palestine was considered for a real case study. The optimization is based on multi-objective genetic algorithm. The obtained results demonstrated the reliability and the cost-effectiveness of the system based on the proposed optimization model.

Based on previous studies, it can be determined that the connection of the hybrid system on the grid is a reliable and cost-effective solution for electrical blackout problems. A proper scheduling program for electrical load shedding could also improve the availability of the main grid energy. The present work has the particularity to combine both hybrid national grid-connected system and a variable load shedding scheduling program to overcome the problem of power outages occurring in the locality of northern Cameroon. Because of the great solar potential in this part of the country, the use of a photovoltaic solar energy system, which is pollution-free, could be a promising alternative solution. The proposed PV/Battery system is used to supply the load not only during blackout periods but also when the grid energy is available. This proposed strategy could allow the reduction in the grid energy consumption and thus the reduction in the energy cost of the system. After presenting the real situation that prevails in this part of Cameroon, a techno-economic study is carried out on the proposed power supply system based on a multi-objective firefly optimization. Several possible scenarios could be envisaged to efficiently meet the electrical demand of households.

2. Presentation of the Current Energy Situation

2.1. Presentation of the Study Area

Cameroon is a country of Central Africa located at the bottom of the Gulf of Guinea, between the 2nd and 13th degrees of north latitude and the 9th and 16th degrees of east longitude. Initially, when the electrical energy production equipment installed in Cameroon were new, the gross production and the consumption were equivalent. However, few years later, a gap was created between production and consumption. Today, this gap has widened considerably due to the failure and aging of the electricity production, transmission, and distribution equipment. Electricity losses have increased, so that households' and companies' electricity demand, which is growing continuously, is not satisfied. Indeed, the country's hydrological resources are amongst the most important in sub-Saharan Africa. Hydroelectricity represents around 77% of the installed capacity [24], but the recent drop in water levels of major dams has lowered this production capacity. As a result, the electricity power supplied remains far below the demand.

Cameroon's natural environment is diverse. It is made up of different natural areas including the northern Sudano-Sahelian part, which is an area of savannas and steppes. Most of this area is characterized by a hot and dry tropical climate with increasingly limited rainfall the closer you get to Lake Chad. The geographical location of the northern part of Cameroon chosen as the study area is presented in Figure 1. The irradiance and ambient temperature data for the three cities that make up this part of Cameroon (Maroua, Garoua, and Ngaoundéré) are presented in Figures 2 and 3 [25].

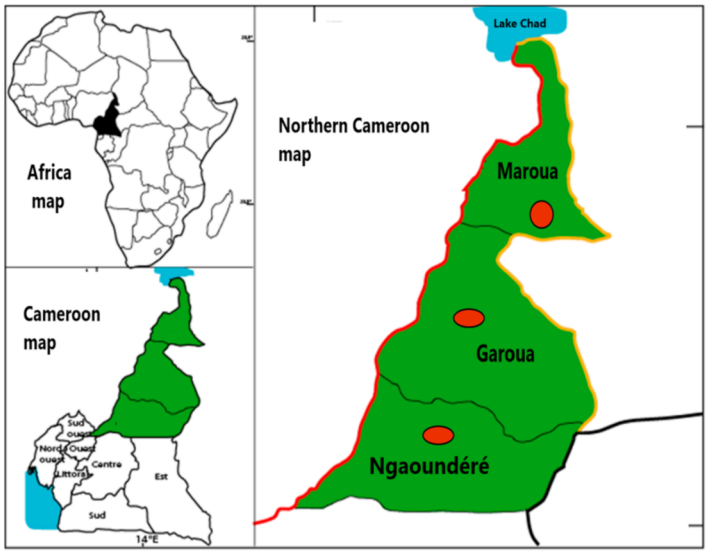

Figure 1. Geographical location of northern Cameroon.

2.2. Current Energy Situation in the Study Area

The northern part of Cameroon is mainly supplied by the Lagdo hydroelectric dam with a total capacity of 72 MW. However, the current production at this plant is estimated at less than 25 MW. Indeed, in October 2019, the volume of water in the Lagdo dam was estimated at 4444 million m^3 of water against 1970 million m^3 of water in October 2020, representing a deficit of 2470 million m^3 of water. Even with the contribution of very expensive—and also very polluting—thermal power plants, the maximum production in this part of Cameroon (less than 45 MW) is not able to meet the electrical demand of the population, estimated to be more than 7,636,555 inhabitants [26]. The current rate of access to electricity is 11.8% for the city of Maroua, 16.6% for the city of Garoua, and 25.5% for the city of Ngaoundéré. While this situation could improve depending on the rainfall recorded, the current energy situation in this part of Cameroon remains a very serious problem for which sustainable solutions must be found independently of rainfall.

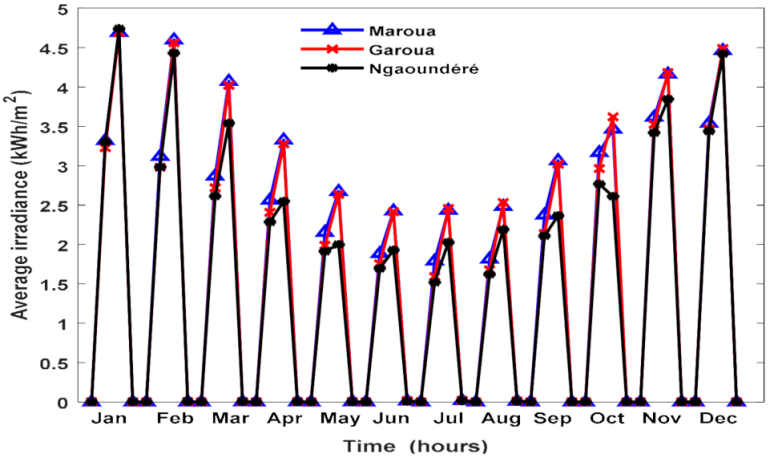

Figure 2. Time variation of irradiance over the year for Maroua, Garoua, and Ngaoundéré. The time variation interval is Δt = 6 h.

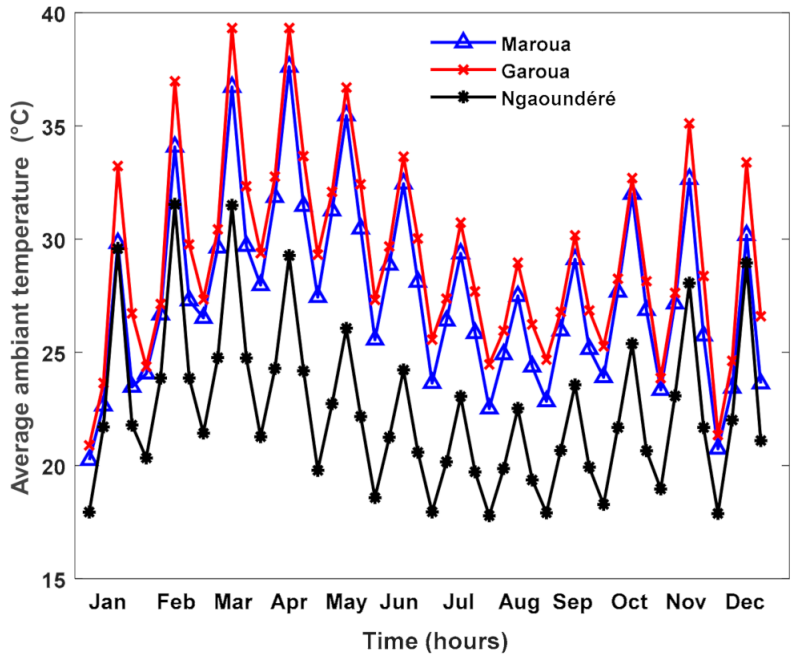

Figure 3. Time variation of ambient temperature over the year for Maroua, Garoua, and Ngaoundéré. The time variation interval is Δt = 6 h.

3. Methodology

3.1. System Modeling

A hybrid system is proposed to solve the load shedding problem encountered in the study site. This hybrid system includes two sources of electrical energy supply (energy from the national interconnection grid and the energy produced by the PV system) for the case of a household whose daily demand is presented in Table 1. A schematic representation of the studied system configuration is given in Figure 4.

Table 1. Estimation of the daily electrical energy demand of one household.

Designation	Quantity	Power (W) Unit	February–May		June–August		September–October		November–January	
			h/d	Wh/d	h/d	Wh/d	h/d	Wh/d	h/d	Wh/d
Lighting	7	9	7	441	7	441	7	441	7	441
Television	1	60	6	360	6	360	6	360	6	360
Radio	1	10	9	90	9	90	9	90	9	90
Ceiling fan	4	45	18	3240	0	0	18	3240	0	0
Computer	2	45	10	900	10	900	10	900	10	900
Refrigerator	1	300	24	7200	24	7200	24	7200	24	7200
Total				12,231		8991		12,231		8991

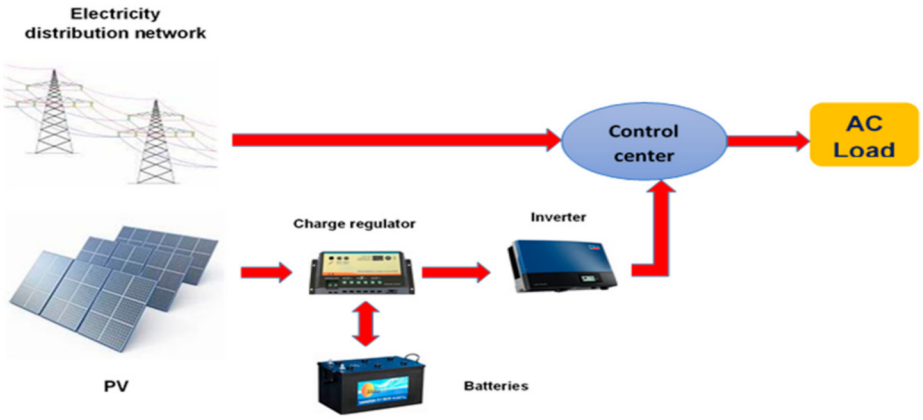

Figure 4. Hybrid PV/Battery/Grid-connected system.

3.1.1. PV Output Model

The PV output is calculated by the equation:

$$E_{pv,out} = N_{pv} \cdot E_{Pv,ref} \cdot \left(\frac{G}{G_{ref}}\right) \cdot \left[1 - \alpha\left(T_c - T_{c,ref}\right)\right] \quad (1)$$

where $E_{pv,ref}$, is the energy of the PV generator corresponding to the standard test conditions.

$$T_c = T_a + \frac{NOCT - 20}{800} \cdot G \quad (2)$$

The total PV electrical energy to supply to the load is given by:

$$E_{pv} = E_{pv,out} \cdot \eta_{inv} \cdot \eta_{regul} \quad (3)$$

3.1.2. Battery Storage Equation Model

The role of batteries is to store the energy produced by the PV generator and to restore this energy when the energy directly supplied by the PV generator is unable to meet the load demand. The storage capacity of batteries is a function of the energy required by the load. Depending on the load and the type of battery used, a photovoltaic installation may require one or more batteries. In a PV installation, the batteries are arranged in series and/or in parallel.

The storage capacity of the batteries can be determined from the following relationship:

$$C_{bat\_max}(Wh) = \frac{N_{ad}(days) \times Maximum\ daily\ load\ energy\ (Wh)}{DOD \times \eta_{batt,c} \times \eta_{inv} \times \eta_{regul}} \quad (4)$$

or

$$C_{bat\_max}(Ah) = \frac{C_{bat\_max}\ (Wh)}{U_n} \quad (5)$$

In the above equations, N_{ad} is the autonomy days of the batteries and U_n is the input/output voltage of the battery bank.

3.1.3. The Main Grid Energy Supply Modeling

The daily electrical energy demand of one household presented in Table 1 depends on the time of the year because some devices such as ceiling fans will not be used when the weather is cold. Figure 5 presents the profile of the daily energy demand of one household depending on the month of the year. Indeed, for an optimal sizing of the system, the present study considers a variable load influenced by the weather conditions. For the periods of the year spanning from February to May and from September to October, the weather is hot and the use of a ceiling fan is necessary. Conversely, for the periods of the year spanning from June to August and from November to January, the weather is cold and there is no need to use a ceiling fan. The use of the ceiling fan increases the load demand.

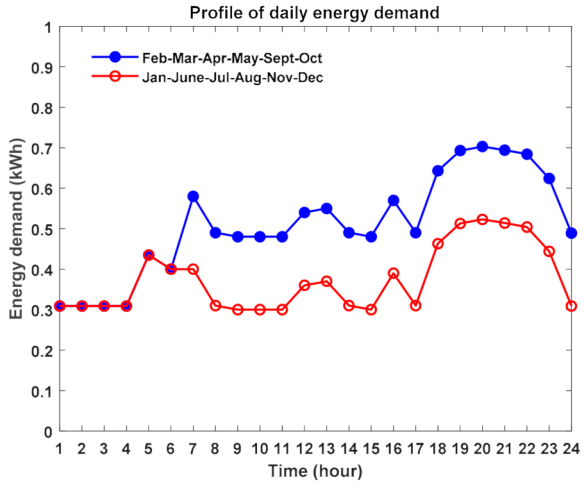

Figure 5. Profile of the daily energy demand for the different months of the year.

In some localities facing the problem of electrical load shedding, there is access programming to the local main grid energy. This program can be daily, weekly, bi-weekly, or even monthly. The objective is to define an automatic programming algorithm for the rotary distribution of energy from the main grid in the case of load shedding over a period of one year. The simulation of the entire electricity production and supply system will be carried out taking into account this annual programming of access to the local energy distribution network.

The electrical energy supplied by the grid is a function of the period of the year since the energy demanded by the load as modeled in this work depends on the month of the year (see Table 1).

In the northern part of Cameroon, over a day of 24 h, the main grid is connected for 6 h (grid energy supply is available) and consecutively disconnected for 6 h (grid energy supply is not available). Thus, to facilitate the simulation of the system, the daily energy demand could be simply defined per time interval of 6 h, as presented in Table 2. Two types of scenarios reflecting the behavior of the connection to the main grid are observed in this part of Cameroon. The two types of scenario occur successively after a duration of 1 week. These two types of scenarios are presented in Table 3. Since the electrical energy demand is not the same over the span of a 24 h day, the main grid energy to supply to the load will depend on the time slots, as defined in Table 3, and therefore it will vary from week to week.

Table 2. Daily energy demand per time interval of 6 h.

Time Variation (Hours)	Δt_1 (1 h–7 h)	Δt_2 (7 h–13 h)	Δt_3 (13 h–19 h)	Δt_4 (19 h–1 h)
Energy demand (kWh) (Feb.-Mar.-Apr.-May-Sept.-Oct.)	2.071	3.050	3.223	3.887
Energy demand (kWh) (Jan.-June-July-Aug.-Nov.-Dec.)	2.071	1.970	2.143	2.807

Table 3. Daily distribution of the connection to the electricity network in a household.

Time Slots	1 h–7 h	7 h–13 h	13 h–19 h	19 h–1 h
Grid connection: week 1	Yes	No	Yes	No
Grid connection: week 2	No	Yes	No	Yes

Let us consider k as the number of the months of the year.

When k = 1, 6, 7, 8, 11, 12, the energy demand could be defined as:

$$D_k = [x_1 \quad x_2 \quad x_3 \quad x_4] \tag{6}$$

When k = 2, 3, 4, 5, 9, 10, the energy demand could be defined as

$$D_k = [x'_1 \quad x'_2 \quad x'_3 \quad x'_4] \tag{7}$$

where x_1, x_2, x_3, x_4, x'_1, x'_2, x'_3, and x'_4 are the energy demands corresponding to each time interval of 6 h over the day.

For two different scenarios of the daily main grid energy supply varying after x number of days over one year, the daily grid energy supply could be defined as follows.

When k = 1, 6, 7, 8, 11, 12:

$$\begin{cases} D_{1,k} = [x_1 \quad 0 \quad x_3 \quad 0] \\ D_{2,k} = [0 \quad x_2 \quad 0 \quad x_4] \end{cases} \tag{8}$$

When k = 2, 3, 4, 5, 9, 10:

$$\begin{cases} D_{1,k} = [x'_1 \quad 0 \quad x'_3 \quad 0] \\ D_{2,k} = [0 \quad x'_2 \quad 0 \quad x'_4] \end{cases} \tag{9}$$

$D_{1,k}$ and $D_{2,k}$ represent the daily main grid energy supply of the month k corresponding to the two different scenarios.

The grid energy supply corresponding to the month k for the combined two types of scenarios each lasting x days could be defined as:

$$\varepsilon_k = [E_{1,k} \quad E_{2,k}] \tag{10}$$

where

$$E_{1,k} = repmat(D_{1,k}, 1, x) \tag{11}$$

and

$$E_{2,k} = repmat(D_{2,k}, 1, x) \tag{12}$$

The monthly grid energy supply is defined as:

$$E_k = [X_1 \quad X_2 \quad X_3 \quad X_4] \tag{13}$$

where

$$X_1 = repmat(D_{2,k}, 1, x - w_{k-1}) \tag{14}$$

$$X_2 = repmat(\varepsilon_k, 1, m_k) \tag{15}$$

$$X_3 = repmat(D_{1,k}, 1, z_k) \tag{16}$$

$$X_4 = repmat(D_{2,k}, 1, w_k) \tag{17}$$

$$z_k + w_k = N_k - x(2m_k + 1) + w_{k-1} \tag{18}$$

In the above equations, w_k, m_k, and z_k are constants to be determined, N_k is the number of the days corresponding to the month k, and *repmat* is a MATLAB (a software produced by Mathworks in USA) function which repeats copies of array.

In Equation (18), if $z_k + w_k \leq x$, then:

$$\begin{cases} z_k = N_k - x(2m_k + 1) + w_{k-1} \\ w_k = 0 \end{cases} \tag{19}$$

If $z_k + w_k < x$, then:

$$\begin{cases} z_k = x \\ w_k = N_k - 2x(m_k + 1) + w_{k-1} \end{cases} \tag{20}$$

m_k is the integer part of the real $(N_k - x + w_{k-1})/2x$.

The annual grid energy supply is given by the array:

$$E_{grid\_annual} = [E_1 \quad E_2 \quad E_3 \quad E_4 \quad E_5 \quad E_6 \quad E_7 \quad E_8 \quad E_9 \quad E_{10} \quad E_{11} \quad E_{12}] \tag{21}$$

Figures 6 and 7 present the daily distribution of the main grid energy supply for the months of January and February, respectively, corresponding to two interchangeable scenarios after a duration of 1 week. For the month of January (corresponding to $k = 1$), the first scenario is defined by $x_1 = 0$, $x_2 = 1.970$, $x_3 = 0$, $x_4 = 2.807$; the second scenario is defined by $x_1 = 2.071$, $x_2 = 0$, $x_3 = 2.143$, $x_4 = 0$. For the month of February (corresponding to $k = 2$), the first scenario is defined by $x'_1 = 0$, $x'_2 = 3.050$, $x'_3 = 0$, $x'_4 = 3.887$; the second scenario is defined by $x'_1 = 2.071$, $x'_2 = 0$, $x'_3 = 3.223$, $x'_4 = 0$. The stars in red color correspond to each 6 h time interval and reflect either the availability of energy or the electrical load shedding (blackouts).

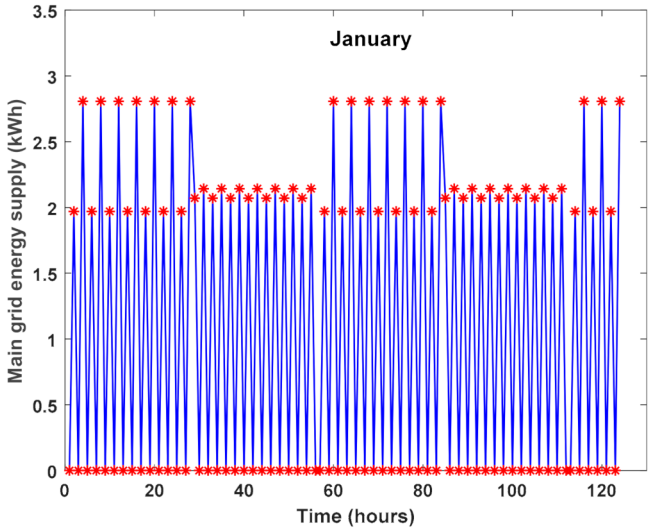

Figure 6. Time variation of the main grid energy supply for the month of January corresponding to two interchangeable scenarios after a duration of 1 week. The first scenario is defined by $x_1 = 0$, $x_2 = 1.970$, $x_3 = 0$, $x_4 = 2.807$; the second scenario is defined by $x_1 = 2.071$, $x_2 = 0$, $x_3 = 2.143$, $x_4 = 0$. The time variation interval is $\Delta t = 6$ h.

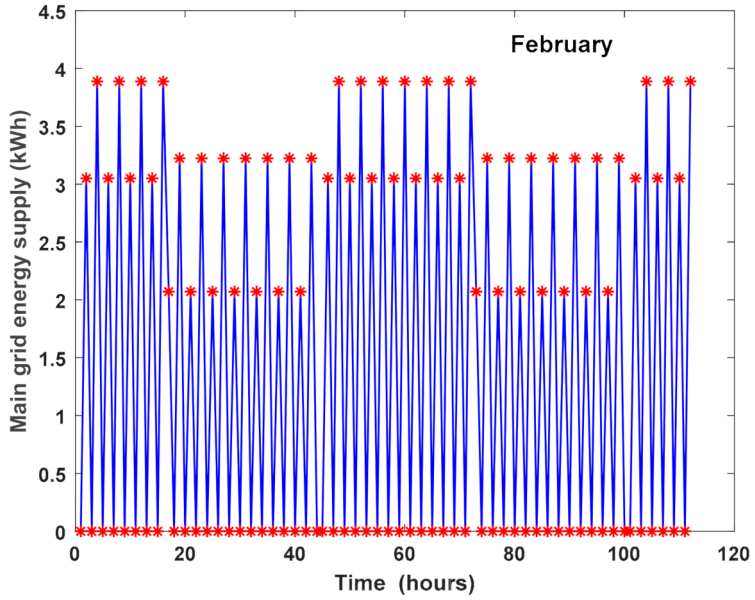

Figure 7. Time variation of the main grid energy supply for the month of February corresponding to two interchangeable scenarios after a duration of 1 week. The first scenario is defined by $x'_1 = 0$, $x'_2 = 3.050$, $x'_3 = 0$, $x'_4 = 3.887$; the second scenario is defined by $x'_1 = 2.071$, $x'_2 = 0$, $x'_3 = 3.223$, $x'_4 = 0$. The time variation interval is $\Delta t = 6$ h.

3.2. System Sizing and Optimization

The Objective Functions

This study is based on a multi-objective optimization to determine the optimal key parameters of the system while minimizing the cost and ensuring an efficient satisfaction of the load energy required. Multi-objective optimization appears as a powerful tool for the optimal sizing of stand-alone PV and hybrid systems [27–35]. Recently, the multi-objective optimization using evolutionary algorithms has emerged as a promising optimization technique for energy systems [28–36]. The most used evolutionary algorithms for energy systems optimization are genetic algorithm and particle swarm optimization methods [28]. However, because of its good and rapid convergence to the solution, this study focused on a multi-objective optimization based on a firefly algorithm [37–40]. The flowchart of the firefly algorithm is presented in Figure 8. The algorithm is used to minimize two objective functions. The first objective function defined by Equation (22) is based on the net present cost (*NPC*) of the energy system, including the initial costs, the installation costs, the operation and maintenance costs, and the replacement costs of the system components. It is given by:

$$fitness(1) = NPC(USD) = Cost_{PV} + Cost_{batteries} + Cost_{inverter} + Cost_{regulator} \quad (22)$$

The second objective function is used to evaluate the system reliability based on the loss of power supply probability (*LPSP*) index. In the case of this study, this index is defined by:

$$fitness(2) = LPSP(\%) = \frac{\sum_{t=1}^{365} hours\left[E_{supply}(\Delta t) < E_d(\Delta t)\right]}{365} \quad (23)$$

Table 4 presents the details concerning the cost and the lifetime of the key components of the studied system used for simulation and matching with the Cameroonian market. These costs include the initial and installation costs. The operation and maintenance for PV module are negligible. For some batteries such as gel batteries, the operation and maintenance costs are also negligible.

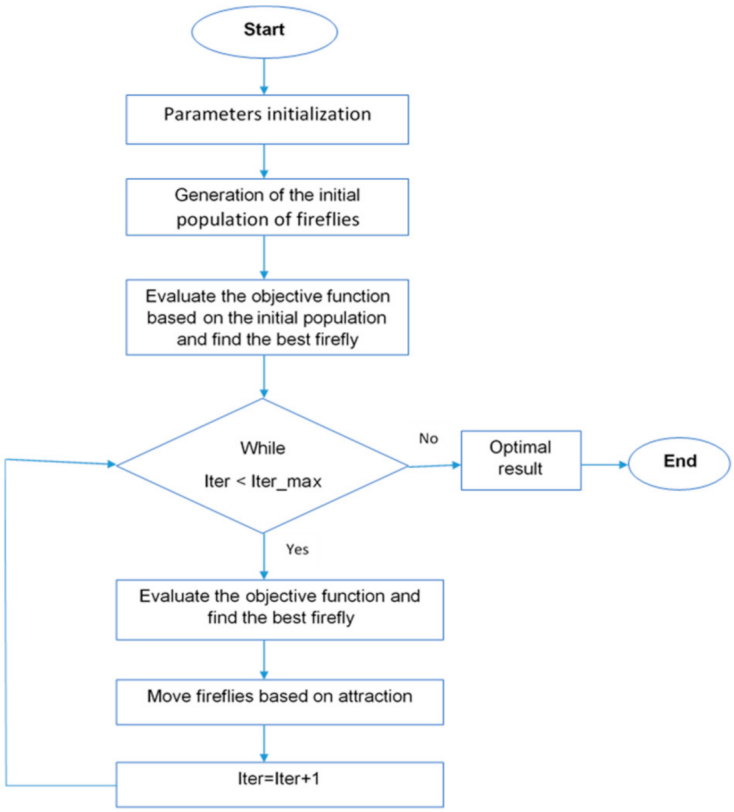

Figure 8. Flowchart of the firefly algorithm.

Table 4. Cost of the key components.

Designation	Unit	Cost (USD)	Lifetime (year)
PV array	W	1	25
Batteries	Ah	1.63	8
Inverter	kW	896	15
Charge regulator	kW	450	15

3.3. Operational Strategy

The primary objective is to use the PV/Battery sub-system to cover the hours of electrical load shedding. However, since these load shedding times are not fixed, we often end up with an overproduction of PV energy. In order to use the most of the available PV energy and thus reduce the cost of consumption of grid energy, in the defined operational strategy, the main grid is sometimes used as a "backup" system. This means that the main grid is requested only when the energy of the PV/Battery subsystem is unable to meet the energy demand.

The operational strategy is described as follows:

1. When the grid connection is on, the grid energy supplies the load and the PV energy system charges the batteries. In this case, the energy charge of batteries and the grid energy supplied at the time interval Δt are given, respectively, by:

$$E_{bat\_c}(\Delta t) = \frac{E_{pv}(\Delta t) \cdot \eta_{bat\_c}}{\eta_{inv} \cdot \eta_{regul}} \tag{24}$$

and

$$E_G(\Delta t) = E_d(\Delta t) \tag{25}$$

The capacity and the state of charge (SOC) of the batteries at the time interval Δt are given, respectively, by:

$$C_{bat}(\Delta t + 1) = C_{bat}(\Delta t) + E_{bat\_c}(\Delta t) \quad (26)$$

and

$$SOC(\Delta t) = \frac{C_{bat}(\Delta t)}{C_{bat\_max}} \quad (27)$$

However, if the PV energy is greater than the maximum allowable battery energy charge ($C_{bat\_max} - C_{batt}(\Delta t)$), then the energy charge of the batteries is:

$$E_{bat\_c}(\Delta t) = \frac{(C_{bat\_max} - C_{bat}(\Delta t)) \cdot \eta_{bat\_c}}{\eta_{inv} \cdot \eta_{regul}} \quad (28)$$

When the batteries are fully charged (SOC (Δt) ≥ 1), the excess energy of the PV system is used to supply the load.

- ➢ If this excess PV energy is greater than or equal to the energy demand, then the grid energy supplied is zero because the total energy demand is satisfied by the PV energy system;
- ➢ Whereas, if the excess PV energy is less than the energy demand, the grid energy supplied is the difference between the energy demand and the PV excess energy:

$$E_G(\Delta t) = E_d(\Delta t) - E_{pv}(\Delta t) \quad (29)$$

2. When the main grid is off, the total energy demand is supplied by the PV system.
   - ➢ If the PV energy is greater than or equal to the energy demand, the surplus PV energy charges the batteries. The energy charge of the batteries at the time interval Δt is then given by:

$$E_{bat\_c}(\Delta t) = \frac{\left(E_{pv}(\Delta t) - E_d(\Delta t)\right) \cdot \eta_{bat\_c}}{\eta_{inv} \cdot \eta_{regul}} \quad (30)$$

If the PV surplus energy is greater than the maximum allowable battery energy charge, then refer to Equation (26) for the battery energy charge equation.

- ➢ If the PV energy is less than the energy demand, the energy deficit is provided by the batteries:
  - If the state of charge of the batteries is less than or equal to the minimum permissible state ($0.2C_{bat\_max}$), the energy discharge of the batteries is zero;
  - If the state of charge of the batteries is greater than the minimum permissible state and if the maximum dischargeable battery energy at the time interval Δt (C_{bat} (Δt) $- 0.2C_{bat\_max}$) is greater than the energy deficit, then the energy supplied by the batteries and the capacity of the batteries at the time t are given by Equations (29) and (30), respectively.

$$E_{bat\_disch}(\Delta t) = E_d(\Delta t) - E_{pv}(\Delta t) \quad (31)$$

$$C_{bat}(\Delta t + 1) = C_{bat}(\Delta t) - \frac{E_d(\Delta t) - E_{pv}(\Delta t)}{\eta_{inv} \cdot \eta_{regul}} \cdot \frac{1}{\eta_{bat\_disch}} \quad (32)$$

  - If the state of charge of the batteries is greater than the minimum permissible state, and if the maximum dischargeable battery energy at the time interval Δt is less than the energy deficit, then the energy supplied by the batteries and the

capacity of the batteries at the time interval Δt are given by Equations (31) and (32), respectively.

$$E_{bat\_disch}(\Delta t) = (C_{bat}(\Delta t) - 0.2C_{bat\_max}) \cdot \eta_{bat\_disch} \cdot \eta_{inv} \quad (33)$$

$$C_{bat}(\Delta t + 1) = C_{bat}(\Delta t) - (C_{bat}(\Delta t) - 0.2C_{bat\_max}) \quad (34)$$

4. Results and Discussion

The hybrid PV/Battery/Grid-connected system considered in this study, taking into account the electrical load shedding, was simulated for three different cities in the northern part of Cameroon. Two different electrical load shedding configurations were taken into account and interchanged after a period of 7 days (1 week), as shown in Table 2. Each day (lasting 24 h) is divided into 4 time slots of 6 h each. These time slots define the periods of availability and non-availability of electrical currents. Indeed, for a 24 h day, electrical energy is available every 6 h of elapsed time, followed by 6 h of electrical blackouts. Each 6 h of unavailability of electrical energy is covered either directly by the PV generator or by the batteries. The Pareto front is used to determine the optimal configurations of the studied system, thus making it possible to define the size of these components. The simulation is performed with a maximum number of 10 iterations and the initial population size (or the number of fireflies) is 1000. In Cameroon, electrical energy supplied by the national electricity distribution company is billed at 79 Fcfa/kWh (Cameroonian currency), or USD 0.15/kWh. Figure 9 shows different optimal solutions obtained depending on the reliability and the investment cost of the system for the cities of Maroua, Garoua, and Ngaoundéré. It emerges from this obtained result that the investment costs of the system are higher in Ngaoundéré compared to Maroua and Garoua. However, a slight difference is observed between the investment costs in Maroua and Garoua. The implementation of this system would be less expensive in Maroua and Garoua compared to Ngaoundéré. However, it is noted in Table 5 (which shows the optimal configuration of the system studied corresponding to *LPSP* of 0% for the three cities considered) that for an *LPSP* of 0%, the investment costs in Maroua and Garoua are equal (of USD 6225.6); this cost is higher in Ngaoundéré (USD 7136.6). Figure 10 presents the monthly time variation interval of PV energy production for the optimal configuration corresponding to *LPSP* of 0% for Maroua, Garoua, and Ngaoundéré. Although the solar potential of Garoua and Maroua is greater than that of Ngaoundéré (see Figure 2), their high ambient temperatures also limit the energy production. There is not much difference between PV energy produced in Maroua and Garoua due to almost similar weather conditions in the two areas. In Figure 10, PV energy production in Ngaoundéré is higher than that of Maroua and Garoua because the number of PV modules for the optimal solution corresponding to *LPSP* of 0% is 10 in Ngaoundéré, while it is eight in both Maroua and Garoua for the same type of module.

A comparison between the energy supply (which is the sum of the PV energy, the discharge energy of the batteries, and the grid energy) and the energy demand is presented in Figures 11–13 for Maroua, Garoua, and Ngaoundéré, respectively. It is shown in these figures that for each time interval over a year, the energy supply is greater than or equal to the energy demand. These results demonstrate the good reliability of the designed systems for the three zones considered where the energy demand is totally satisfied.

The energy balance of the entire hybrid system for each month of the year in the three study areas is presented in Table 6. It emerges from this balance that the monthly demand for electrical energy is fully satisfied in the three cities considered despite the load shedding phenomenon.

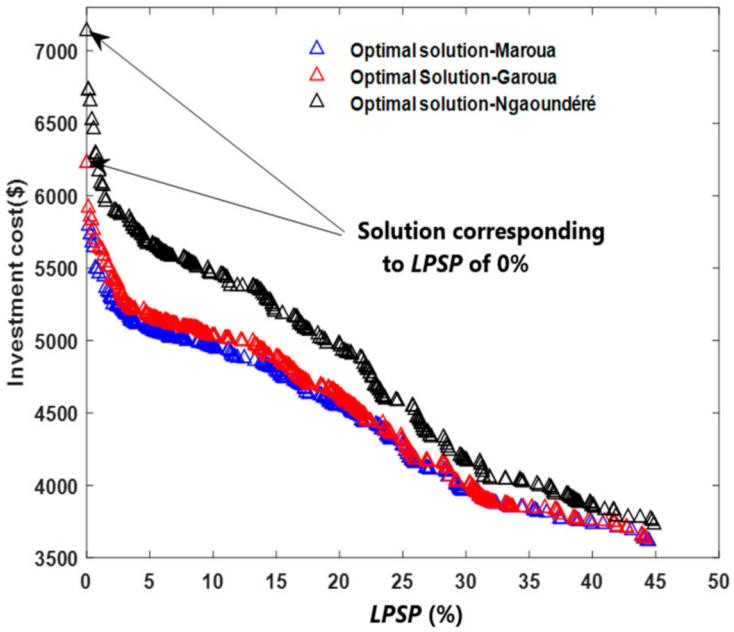

Figure 9. Pareto front solutions based on a double-objective optimization.

Table 5. Optimal system configuration corresponding to *LPSP* of 0% for different cities.

City	*LPSP* (%)	Number of PV Modules	Autonomy of Batteries (Days)	Capacity of Batteries (kWh)	Investment Cost (USD)
Maroua	0	8	1	11.304	6225.6
Garoua	0	8	1	11.304	6225.6
Ngaoundéré	0	10	1	11.304	7136.6

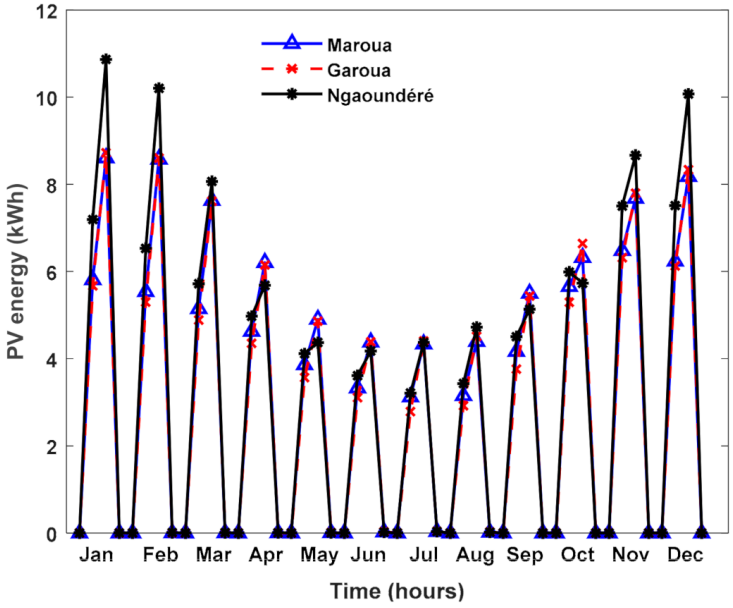

Figure 10. Time variation of PV energy production over the year for the optimal configuration corresponding to *LPSP* of 0%. The time variation interval is Δt = 6 h.

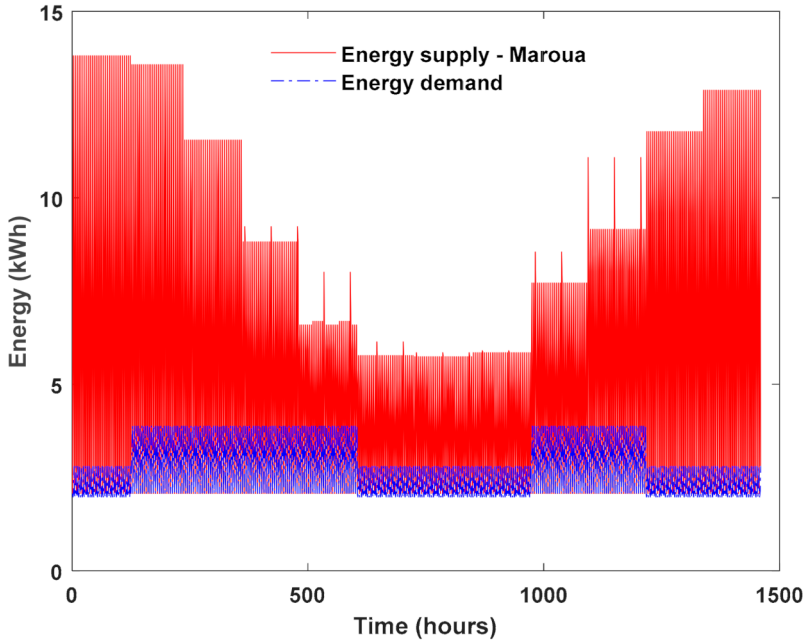

Figure 11. Comparison between 1-year time variation of energy supply (PV energy supply + discharge energy of batteries + grid connection energy supply) and energy demand for the optimal configuration corresponding to *LPSP* of 0%, in the case of Maroua. The time variation interval is Δt = 6 h.

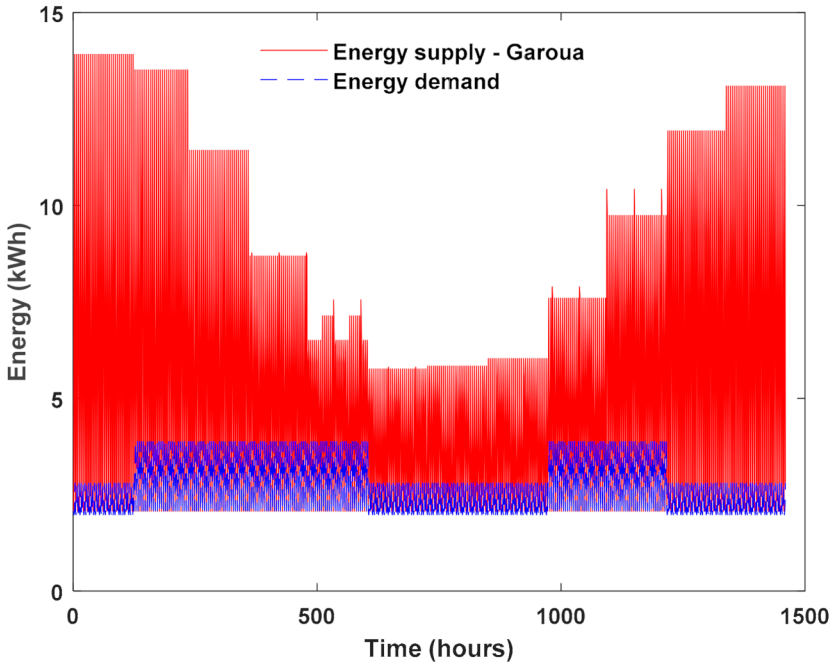

Figure 12. Comparison between one year time variation of energy supply (PV energy supply + discharge energy of batteries + grid connection energy supply) and energy demand for the optimal configuration corresponding to *LPSP* of 0%, in the case of Garoua. The time variation interval is Δt = 6 h.

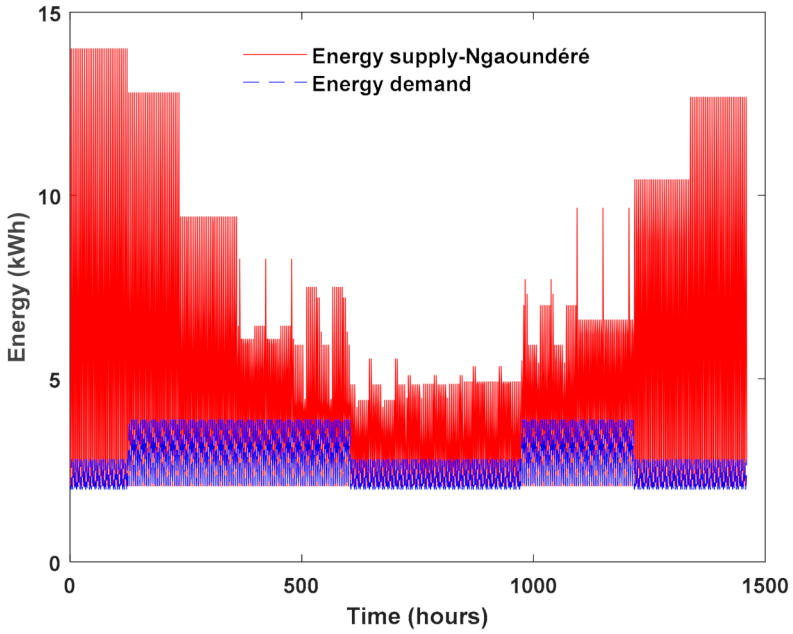

Figure 13. Comparison between one year time variation of energy supply (PV energy supply + discharge energy of batteries + grid connection energy supply) and energy demand for the optimal configuration corresponding to *LPSP* of 0%, in the case of Ngaoundéré. The time variation interval is Δt = 6 h.

Table 7 presents the monthly contribution of each energy supply component of the system to the total energy consumed. For the town of Maroua, the contribution of the main grid is between 27.453% and 44.615%, the direct contribution of the PV generator is between 31.772% and 48.197%, and the contribution of the battery storage is between 23.612% and 27.523%. Since the energy supplied by the batteries is typically provided by the PV generator, the PV energy represents 60.385% to 72.546% of the energy demand (load consumed). For the town of Garoua, the contribution of the main grid is between 28.144% and 47.031%, the direct contribution of the PV generator is between 29.363% and 47.379%, and the contribution of the battery storage is between 23.605% and 27.523%. The PV energy represents from 58.371% to 71.855% of the energy demand (load consumed). For the town of Ngaoundéré, the contribution of the main grid is between 25.839% and 44.985%, the direct contribution of the PV generator is between 31.391% and 49.575%, and the contribution of the battery storage is between 23.622% and 27.510%. The PV energy represents from 61.233% to 74.160% of the energy demand (load consumed). Based on the proposed operational strategy for cost reduction, the obtained results from Table 7 show that the main energy supply component in a PV/Grid-connected system submitted to variable load shedding is the PV generator.

Table 8 presents the monthly percentage of surplus of energy released by the PV generator. This energy is lost by the system. The average annual energy lost by the system represents 34.439%, 34.556%, and 36.741% of the total PV energy produced in Maroua, Garoua, and Ngaoundéré, respectively. The amount of energy lost could be reduced by increasing the battery storage size, thus resulting in a reduction in the main grid energy demand contribution. Although this solution could reduce the main grid energy consumed cost, it could also increase the battery storage cost. Another alternative to harness the excess PV energy produced would be to sell this energy to the nearest users.

Table 9 presents a comparison of the total energy investment cost between an autonomous main grid system without electrical load shedding, an autonomous system main grid system with electrical load shedding, and a hybrid system combining the main grid with electrical load shedding and the PV energy system. For a lifespan of the system of 25 years, the autonomous main grid with electrical load shedding will always be the least

expensive system but will not be able to meet the energy demand in the cities considered. At the initial investment, the stand-alone main grid system without power shedding is more cost effective compared to the hybrid PV/Battery/Grid-connected system with power shedding. However, the hybrid PV/Battery Grid-connected system with electrical load shedding becomes more economically advantageous from the 17th year for the city of Maroua, and the 18th year for both the cities of Garoua and Ngaoundéré. Thus, for a long-term investment, the hybrid PV/Battery/Grid-connected system is economically more profitable. Indeed, this conclusion is the same made by previous works [9,10]. It can be seen in Figure 14 that the optimal hybrid system required to cover the household energy demand in Ngaoundéré is more expensive compared to Maroua and Garoua for the same energy demand. The system investment costs are almost the same in Maroua and Garoua, although Maroua has a slightly lower investment cost advantage than Garoua.

Table 6. Energy balance of the system for each month of the year.

City	Month (mth)	E_d (kWh)	E_G (kWh)	$E_{PV,s}$ (kWh)	$E_{pv,c}$ (kWh)	$E_{b,d}$ (kWh)	$E_s = E_G + E_{pv,c} + E_{b,d}$ (kWh)	$E_{surplus} = E_{pv,s} - E_{pv,c} - E_{b,d}$ (kWh)
Maroua	January	278.721	78.445	446.970	123.563	76.713	278.721	246.694
	February	342.468	94.019	395.270	165.061	83.388	342.468	146.821
	March	379.161	104.898	396.260	179.279	94.984	379.161	121.997
	April	366.930	125.821	325.020	151.818	89.291	366.930	83.911
	May	379.161	169.164	271.820	120.469	89.528	379.161	61.823
	June	269.730	102.668	231.940	94.941	72.121	269.730	64.878
	July	278.721	110.412	232.310	93.553	74.756	278.721	64.001
	August	278.721	105.078	234.370	97.217	76.426	278.721	60.727
	September	366.930	143.614	289.890	132.130	91.186	366.960	66.574
	October	379.161	107.878	371.240	181.658	89.625	379.161	99.957
	November	269.730	76.374	424.740	119.450	73.906	269.730	231.384
	December	278.721	81.151	446.870	121.593	75.977	278.721	249.300
Garoua	January	278.721	78.445	446.150	123.563	76.713	278.721	245.874
	February	342.468	96.869	389.341	162.260	83.339	342.468	143.742
	March	379.161	107.983	387.659	176.224	94.954	379.161	116.481
	April	366.930	133.995	315.216	143.644	89.291	366.930	82.281
	May	379.161	178.326	261.487	111.333	89.502	379.161	60.652
	June	269.730	107.785	225.551	89.899	72.046	269.730	63.606
	July	278.721	116.028	224.184	88.019	74.674	278.721	61.491
	August	278.721	108.781	231.080	93.604	76.336	278.721	61.140
	September	366.930	154.133	275.978	121.639	91.158	366.930	63.181
	October	379.161	112.949	369.930	176.587	89.625	379.161	103.718
	November	269.730	76.374	423.488	119.450	73.906	269.730	230.132
	December	278.721	81.151	448.428	121.593	75.977	278.721	250.858
Ngaoundéré	January	278.721	77.529	559.851	124.514	76.678	278.721	358.659
	February	342.468	89.394	468.794	169.780	83.294	342.468	215.720
	March	379.161	97.973	427.605	186.259	94.929	379.161	146.417
	April	366.930	124.216	319.846	153.439	89.275	366.930	77.132
	May	379.161	170.568	263.116	119.026	89.567	379.161	54.523
	June	269.730	98.434	234.205	99.124	72.172	269.730	62.909
	July	278.721	108.049	236.098	95.928	74.744	278.721	65.426
	August	278.721	96.235	253.322	106.089	76.397	278.721	70.836
	September	366.930	140.516	289.226	135.228	91.186	366.930	62.812
	October	379.161	104.223	363.278	185.313	89.625	379.161	88.340
	November	269.730	74.873	485.050	120.951	73.906	269.730	290.193
	December	278.721	78.866	545.147	123.878	75.977	278.721	345.292

The marked numbers in blue, red and green color indicate how the energy demand is fully satisfied by the energy supply respectively in Maroua, Garoua and Ngaoundéré.

Table 7. Monthly contribution of each energy supply component of the system to the total energy consumed.

City	Month	E_d (kWh)	E_G (kWh)	$E_{pv,c}$ (kWh)	$E_{b,d}$ (kWh)	E_G/E_d (%)	$E_{pv,c}/E_d$ (%)	$E_{b,d}/E_d$ (%)	*PV + Batt* (%)
Maroua	January	278.721	78.445	123.563	76.713	28.144	44.332	27.523	71.855
	February	342.468	94.019	165.061	83.388	27.453	48.197	24.349	72.546
	March	379.161	104.898	179.279	94.984	27.665	47.282	25.051	72.334
	April	366.930	125.821	151.818	89.291	34.290	41.375	24.334	65.709
	May	379.161	169.164	120.469	89.528	44.615	31.772	23.612	55.384
	June	269.730	102.668	94.941	72.121	38.063	35.198	26.738	61.936
	July	278.721	110.412	93.553	74.756	39.614	33.565	26.820	60.385
	August	278.721	105.078	97.217	76.426	37.700	34.879	27.42	62.299
	September	366.930	143.614	132.130	91.186	39.139	36.009	24.851	60.860
	October	379.161	107.878	181.658	89.625	28.451	47.910	23.637	71.548
	November	269.730	76.374	119.450	73.906	28.314	44.285	27.399	71.685
	December	278.721	81.151	121.593	75.977	29.115	43.625	27.259	70.884
Garoua	January	278.721	78.445	123.563	76.713	28.144	44.332	27.523	71.855
	February	342.468	96.869	162.260	83.339	28.285	47.379	24.334	71.714
	March	379.161	107.983	176.224	94.954	28.479	46.477	25.043	71.520
	April	366.930	133.995	143.644	89.291	36.517	39.147	24.334	63.482
	May	379.161	178.326	111.333	89.502	47.031	29.363	23.605	52.968
	June	269.730	107.785	89.899	72.046	39.960	33.329	26.710	60.039
	July	278.721	116.028	88.019	74.674	41.628	31.579	26.791	58.371
	August	278.721	108.781	93.604	76.336	39.028	33.583	27.387	60.971
	September	366.930	154.133	121.639	91.158	42.006	33.150	24.843	57.993
	October	379.161	112.949	176.587	89.625	29.789	46.573	23.637	70.210
	November	269.730	76.374	119.450	73.906	28.314	44.285	27.399	71.685
	December	278.721	81.151	121.593	75.977	29.115	43.625	27.259	70.884
Ngaoundéré	January	278.721	77.529	124.514	76.678	27.815	44.673	27.510	72.184
	February	342.468	89.394	169.780	83.294	26.102	49.575	24.321	73.897
	March	379.161	97.973	186.259	94.929	25.839	49.124	25.036	74.160
	April	366.930	124.216	153.439	89.275	33.852	41.816	24.330	66.147
	May	379.161	170.568	119.026	89.567	44.985	31.391	23.622	55.014
	June	269.730	98.434	99.124	72.172	36.493	36.749	26.757	63.506
	July	278.721	108.049	95.928	74.744	38.766	34.417	26.816	61.233
	August	278.721	96.235	106.089	76.397	34.527	38.062	27.409	65.472
	September	366.930	140.516	135.228	91.186	38.294	36.853	24.851	61.705
	October	379.161	104.223	185.313	89.625	27.487	48.874	23.637	72.512
	November	269.730	74.873	120.951	73.906	27.758	44.841	27.399	72.241
	December	278.721	78.866	123.878	75.977	28.295	44.444	27.259	71.704

In each column, the marked numbers in color represent the minimum and the maximum percentage of energy contribution of the different components of the system. Blue color is used for the town of Maroua, red color is used for the town of Garoua and green color is used for the town of Ngaoundéré.

Table 8. Percentage of surplus of energy released by the PV generator.

Month	$E_{pv,s}/E_{surplus\_maroua}$ (%)	$E_{pv,s}/E_{surplus\_garoua}$ (%)	$E_{pv,s}/E_{surplus\_ngaoundéré}$ (%)
January	55.192	55.110	64.063
February	37.144	36.919	46.015
March	30.787	30.047	34.241
April	25.817	26.103	24.115
May	22.744	23.194	20.722
June	27.972	28.200	26.860
July	27.550	27.428	27.711
August	25.911	26.458	27.963
September	22.965	22.893	21.717
October	26.925	28.037	24.317
November	54.476	54.342	59.827
December	55.788	55.941	63.339
Annual average percentage of surplus of energy (%)	34.439	34.556	36.741

Table 9. Comparison of the total energy investment cost between different energy supply configurations.

Energy Supply Configuration		Only Grid Connection without Power Shedding		Only Grid Connection with Power Shedding		PV Energy Production System	Grid Connection with Power Shedding + PV System
City	Year	Energy Consumed (kWh)	Total Cost of Energy (USD)	Energy Consumed (kWh)	Total Cost of Energy (USD)	Total Investment Cost (USD)	Total Cost (USD)
Maroua	1	3868.155	558.736	1299.524	187.710	6225.6	6413.310
	2	7736.310	1117.473	2599.049	375.420	6225.6	6601.020
	3	11,604.465	1676.209	3898.573	563.130	6225.6	6788.730
	4	15,472.62	2234.946	5198.098	750.840	6225.6	6976.440
	5	19,340.775	2793.683	6497.622	938.550	6225.6	7164.150
	6	23,208.93	3352.419	7797.147	1126.260	6225.6	7351.860
	7	27,077.085	3911.156	9096.671	1313.971	6225.6	7539.571
	8	30,945.24	4469.893	10,396.196	1501.681	6225.6	7727.281
	9	34,813.395	5028.629	11,695.720	1689.391	6225.6	7914.991
	10	38,681.550	5587.366	12,995.245	1877.101	6225.6	8102.701
	11	42,549.705	6146.103	14,294.769	2064.811	6225.6	8290.411
	12	46,417.860	6704.839	15,594.294	2252.521	6225.6	8478.121
	13	50,286.015	7263.576	16,893.818	2440.231	6225.6	8665.831
	14	54,154.170	7822.313	18,193.343	2627.942	6225.6	8853.542
	15	58,022.325	8381.049	19,492.867	2815.652	6225.6	9041.252
	16	61,890.480	8939.786	20,792.392	3003.362	6225.6	9228.962
	17	65,758.635	9498.522	22,091.916	3191.072	6225.6	9416.672
	18	69,626.790	10,057.259	23,391.441	3378.782	6225.6	9604.382
	19	73,494.945	10,615.996	24,690.965	3566.492	6225.6	9792.092
	20	77,363.100	11,174.732	25,990.490	3754.203	6225.6	9979.803
	21	81,231.255	11,733.469	27,290.014	3941.913	6225.6	10,167.513
	22	85,099.410	12,292.206	28,589.539	4129.623	6225.6	10,355.223
	23	88,967.565	12,850.942	29,889.063	4317.333	6225.6	10,542.933
	24	92,835.720	13,409.679	31,188.588	4505.043	6225.6	10,730.643
	25	96,703.875	13,968.416	32,488.112	4692.753	6225.6	10,918.353
Garoua	1	3868.155	558.736	1352.818	195.408	6225.6	6421.008
	2	7736.310	1117.473	2705.636	390.816	6225.6	6616.416
	3	11,604.465	1676.209	4058.455	586.224	6225.6	6811.824
	4	15,472.620	2234.946	5411.273	781.632	6225.6	7007.232
	5	19,340.775	2793.683	6764.092	977.041	6225.6	7202.641
	6	23,208.930	3352.419	8116.910	1172.449	6225.6	7398.049
	7	27,077.085	3911.156	9469.728	1367.857	6225.6	7593.457
	8	30,945.240	4469.893	10,822.547	1563.265	6225.6	7788.865
	9	34,813.395	5028.629	12,175.365	1758.673	6225.6	7984.273
	10	38,681.550	5587.366	13,528.184	1954.082	6225.6	8179.682
	11	42,549.705	6146.103	14,881.002	2149.490	6225.6	8375.090
	12	46,417.860	6704.839	16,233.820	2344.898	6225.6	8570.498
	13	50,286.015	7263.576	17,586.639	2540.306	6225.6	8765.906
	14	54,154.170	7822.313	18,939.457	2735.714	6225.6	8961.314
	15	58,022.325	8381.049	20,292.276	2931.123	6225.6	9156.723
	16	61,890.480	8939.786	21,645.094	3126.531	6225.6	9352.13
	17	65,758.635	9498.522	22,997.912	3321.939	6225.6	9547.539
	18	69,626.790	10,057.259	24,350.731	3517.347	6225.6	9742.947
	19	73,494.945	10,615.996	25,703.549	3712.755	6225.6	9938.355
	20	77,363.100	11,174.732	27,056.368	3908.164	6225.6	10,133.764
	21	81,231.255	11,733.469	28,409.186	4103.572	6225.6	10,329.172
	22	85,099.410	12,292.206	29,762.004	4298.980	6225.6	10,524.580
	23	88,967.565	12,850.942	31,114.823	4494.388	6225.6	10,719.988
	24	92,835.720	13,409.679	32,467.641	4689.796	6225.6	10,915.396
	25	96,703.875	13,968.416	33,820.460	4885.205	6225.6	11,110.805
Ngaoundéré	1	3868.155	558.736	1260.876	182.127	7136.6	7318.727
	2	7736.310	1117.473	2521.752	364.255	7136.6	7500.855
	3	11,604.465	1676.209	3782.629	546.382	7136.6	7682.982
	4	15,472.620	2234.946	5043.505	728.510	7136.6	7865.110
	5	19,340.775	2793.683	6304.382	910.638	7136.6	8047.238
	6	23,208.930	3352.419	7565.258	1092.765	7136.6	8229.365
	7	27,077.085	3911.156	8826.134	1274.893	7136.6	8411.493
	8	30,945.240	4469.893	10087.011	1457.020	7136.6	8593.620
	9	34,813.395	5028.629	11,347.887	1639.148	7136.6	8775.748
	10	38,681.550	5587.366	12,608.764	1821.276	7136.6	8957.876
	11	42,549.705	6146.103	13,869.640	2003.403	7136.6	9140.003
	12	46,417.860	6704.839	15,130.516	2185.531	7136.6	9322.131
	13	50,286.015	7263.576	16,391.393	2367.659	7136.6	9504.259
	14	54,154.170	7822.313	17,652.269	2549.786	7136.6	9686.386
	15	58,022.325	8381.049	18,913.146	2731.914	7136.6	9868.514
	16	61,890.480	8939.786	20,174.022	2914.041	7136.6	10,050.641
	17	65,758.635	9498.522	21,434.898	3096.169	7136.6	10,232.769
	18	69,626.790	10,057.259	22,695.775	3278.297	7136.6	10,414.897
	19	73,494.945	10,615.996	23,956.651	3460.424	7136.6	10,597.024
	20	77,363.100	11,174.732	25,217.528	3642.552	7136.6	10,779.152
	21	81,231.255	11,733.469	26,478.404	3824.679	7136.6	10,961.279
	22	85,099.410	12,292.206	27,739.280	4006.807	7136.6	11,143.407
	23	88,967.565	12,850.942	29,000.157	4188.935	7136.6	11,325.535
	24	92,835.720	13,409.679	30,261.033	4371.062	7136.6	11,507.662
	25	96,703.875	13,968.416	31,521.910	4553.190	7136.6	11,689.790

The marked rows in color represent the time when the hybrid PV/Battery/Grid-connected system becomes more advantageous than the only grid without electrical blackouts. The blue, red and green colors are used to indicate this time respectively for the towns of Maroua, Garoua and Ngaoundéré.

Although the proposed PV/Battery system connected to an unreliable electric grid to face the problem of electrical blackouts is efficient, clean, and economically feasible, it is, however, still very expensive in the short term compared to other proposed solutions, such as the diesel generator grid-connected system [13]. Likewise, it emerges from this work that the energy consumption of a PV/Battery/Grid-connected system with electrical load shedding is for the users more expensive than the energy consumption of the main electric grid without electrical load shedding or blackouts, this for an investment over a period of 17 years maximum. This is to say that, in this context, the PV/Battery system, although allowing a reduction in the grid energy consumption, makes the cost of energy more expensive for the user while ensuring continuous availability and satisfactory energy

to the load. It is the concern to make the system 100% reliable that increases its investment cost, also resulting in an increase in the excess of PV energy produced since the distribution of the energy demand is disproportionate. The grid energy consumed could be further reduced by using this excess energy from a storage system that is relatively less expensive than batteries to allow a net decrease in the investment cost and thus allow the system to be economically more competitive. If, for example, the electrical blackouts were planned only during the day, the excess PV energy produced, which is also a function of solar irradiation, would be considerably reduced.

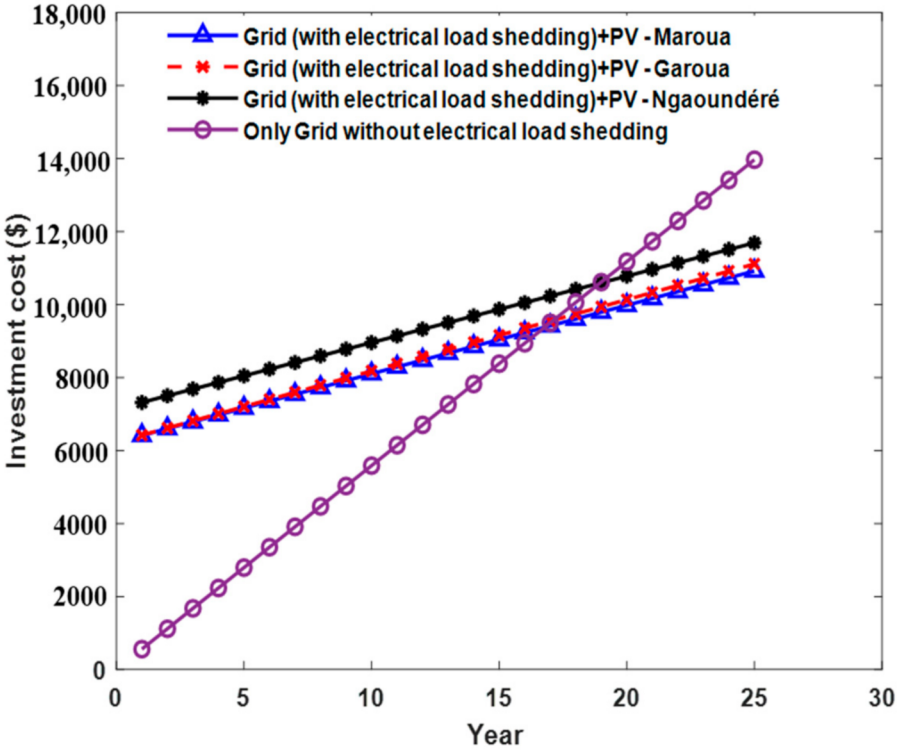

Figure 14. Comparison of the total investment cost between the hybrid PV/Battery/Grid-connected system and the only main grid (without electrical load shedding) for the sites of Maroua, Garoua, and Ngaoundéré.

The rotary variation of the electrical load shedding scheduling program between users (as carried out by the national electricity distribution company of Cameroon) leads to a sizing of the PV system so that the total energy produced is greater than or equal to the grid energy consumed by the load in the absence of any electrical blackouts. Thus, the PV/Battery system sized and corresponding to an *LPSP* of 0% would be technically able to meet the load requirement on its own, which will, however, require a fairly large storage system and therefore an increase in the investment cost, which will no longer be only USD 6225.6 for Maroua and Garoua and USD 7136.6 for Ngaoundéré, but much more. It is therefore difficult to predict that the stand-alone PV/Battery system would be economically more advantageous than the electric grid alone without blackouts. However, as demonstrated in this work, with regard to the PV/Battery system connected to the grid, it is competitive in the long term. It comes out that a proper load shedding scheduling strategy for the users could economically improve the PV/Battery/Grid-connected system in the presence of electrical blackouts.

5. Conclusions

The objective of this work was to propose an effective solution to the problems of electrical load shedding encountered by some populations of the world in general and of northern Cameroon, in particular. This solution consists of connecting a PV system

to the local main grid. The hybrid system formed is able to respond efficiently to the requested energy demand. Thanks to a double objective optimization based on a defined operational strategy, the optimal system configurations were determined. A method of annual evaluation of the daily energy supplied by the grid per time interval according to its availability and the energy demand was carried out in this work. The energy supplied by the PV system not only helps fill off-peak hours without electricity, but also reduces grid energy consumption even when the grid energy is available. A comparative cost study was carried out between the hybrid PV/Grid system and the grid system without power shedding. It was found that for a certain period of time, the cost of grid energy consumed by the load is less expensive than the cost of energy consumed from the PV/Grid-connected system. However, from the 17th year of consumption, the PV/Grid-connected system becomes economically more profitable in the case of the city of Maroua and from the 18th year in the case of the cities of Garoua and Ngaoundéré. Thus, for a long-term investment, the PV/Battery/Grid-connected system is economically more advantageous. As demonstrated in this work, it is certain that the implementation of the PV/Battery/Grid-connected system is an effective solution to circumvent the problem of electrical load shedding (electrical blackouts), which negatively influences the socio-economic life of some populations. Developing in the near future a proper scheduling program for electrical blackouts could improve the system both technically and economically.

Author Contributions: Conceptualization, investigation, and writing, R.Z.F.; resources, F.N.W., V.D; validation, V.D., C.B.S. and A.D.; supervision, V.D., N.D. and S.Y.D.; revision, R.Z.F. and S.Y.D. All authors have read and agreed to the published version of the manuscript.

Funding: This research received no external funding.

Institutional Review Board Statement: Not applicable.

Informed Consent Statement: Not applicable.

Data Availability Statement: Data sharing not applicable.

Conflicts of Interest: The authors declare no conflict of interest.

Nomenclature

Abbreviations

PV	Photovoltaic
NOCT	Nominal operating cells temperature (°C)
SOC	State of charge of water in the reservoir
LPSP	Loss of power supply probability
NPC	Net present cost
FA	Firefly algorithm

Symbols

N_{pv}	Number of photovoltaic modules
$E_{pv,out}$	Photovoltaic energy production (kW)
E_{pv}	Photovoltaic energy supplied (kW)
$E_{pv,ref}$	Photovoltaic energy at reference condition (25 °C or 298 K) (kW)
T_a	Ambient temperature (°C)
G	Solar radiation (kWh/m^2)
G_{ref}	Irradiance at reference condition (kW/m^2)
G_{NOCT}	Solar radiation at NOCT (kWh/m^2)
T_c	Cell temperature (°C or K)
$T_{c,ref}$	Cell temperature at reference condition (25 °C or 298 K)
E_{pv}	Photovoltaic daily energy production
Iter	Iteration
Iter_max	Maximum number of iterations
C_{bat}	Storage capacity of batteries (kWh or kAh)

C_{bat_max}	Maximum storage capacity of batteries (kWh or kAh)
U_n	Nominal voltage of battery bank (V)
E_{bat_c}	Energy of charge of batteries (kWh)
E_{bat_disch}	Energy of discharge of batteries (kWh)
$E_{pv,s}$	PV energy supplied (kWh)
$E_{pv,c}$	PV energy consumed (kWh)
E_s	Energy supplied to load (kWh)
$E_{surplus}$	Surplus of enery (kWh)
$E_{surplus\_maroua}$	Monthly surplus of energy corresponding to Maroua
$E_{surplus\_garoua}$	Monthly surplus of energy corresponding to Garoua
$E_{surplus\_ngaoundéré}$	Monthly surplus of energy corresponding to Ngaoundéré
$E_{b,d}$	Battery energy discharged (kWh)
C_{batt}	Storage capacity of batteries (kWh or kAh)
E_{supply}	Energy supplied to load
E_d	Energy demand
E_G	Grid energy supplied
N_{ad}	Number of autonomy days of batteries
$Cost_{pv}$	Cost of photovoltaic modules
$Cost_{reservoir}$	Cost of reservoir
$Cost_{regulator}$	Cost of regulator
Greek symbols	
α	Temperature coefficient of short-circuit current (A/K)
η_{inv}	Inverter efficiency
η_{regul}	Regulator efficiency
η_{bat_c}	Efficiency of charge of batteries (%)
η_{bat_disch}	Efficiency of discharge of batteries (%)
USD	American US dollar

References

1. World Economic Forum. Available online: https://www.weforum.org/agenda/2019/05/patchy-progress-on-electricity-access-casts-shadow-on-global-goal (accessed on 25 March 2021).
2. Husna, S.; Abdullah, M.P.; Faridiansyah, I. An improved load shedding scheduling strategy for solving power supply defisit. *J. Teknol.* **2016**, *78*, 5–7.
3. Hirodontis, S.; Li, H.; Crossley, P.A. Load shedding in a distribution network. In Proceedings of the International Conference on Sustainable Power Generation and Supply, Nanjing, China, 6–7 April 2009.
4. Faranda, R.; Pievatolo, A.; Tironi, E. Load shedding: A new proposal. *IEEE Trans. Power Syst.* **2007**, *22*, 2086–2093. [CrossRef]
5. Crampes, C.; Léautier, T.O. Distributed load-shedding in the balancing of electricity markets. In Proceedings of the 9th International Conference on the European Energy Market, Florence, Italy, 10–12 May 2012.
6. Emar, W.; Al-Barami, G.S. Economical Motivation and Benefits of using Load Shedding in Energy Management Systems. *Int. J. Adv. Comput. Sci. Appl.* **2019**, *10*, 204–209. [CrossRef]
7. Margaret, V.; Rao, K.U.; Ganeshprasad, G.G. Intelligent load shedding using ant colony algorithm in smart grid environment. *Power Electron. Renew. Energy Syst.* **2015**, 1149–1162. [CrossRef]
8. Ullah, I.; Rasheed, M.B.; Alquthami, T.; Tayyaba, S. A Residential Load Scheduling with the Integration of On-Site PV and Energy Storage Systems in Micro-Grid. *Sustainability* **2019**, *12*, 184. [CrossRef]
9. Alramlawi, M.; Gabash, A.; Mohagheghi, E.; Li, P. Optimal operation of hybrid PV-battery system considering grid scheduled blackouts and battery lifetime. *Solar Energy* **2018**, *161*, 125–137. [CrossRef]
10. Bastholm, C.; Fiedler, F. Techno-economic study of the impact of blackouts on the viability of connecting an off-grid PV-diesel hybrid system in Tanzania to the national power grid. Bastholm, Caroline, and Frank Fiedler. Techno-economic study of the impact of blackouts on the viability of connecting an off-grid PV-diesel hybrid system in Tanzania to the national power grid. *Energy Convers. Manag.* **2018**, *171*, 647–658.
11. Alibakhsh, K.; Rahdan, P.; Rad, M.A.V.; Yan, W.M. Optimal design and technical analysis of a grid-connected hybrid photovoltaic/diesel/biogas under different economic conditions: A case study. *Energy Convers. Manag.* **2019**, *198*, 111810.
12. Samy, M.M.; Mosaad, M.I.; Barakat, S. Optimal economic study of hybrid PV-wind-fuel cell system integrated to unreliable electric utility using hybrid search optimization technique. *Int. J. Hydrog. Energy* **2021**, *46*, 11217–11231. [CrossRef]
13. Murphy, P.M.; Ssennoga, T.; Murphy, I.S. Analysis of the cost of reliable electricity: A new method for analyzing grid connected solar, diesel and hybrid distributed electricity systems considering an unreliable electric grid, with examples in Uganda. *Energy* **2014**, *66*, 523–534. [CrossRef]

14. Saleh, A.A.; NaimTajuddin, M.F.; Adzman, M.R.; Mohammed, M.F.; Ramli, M.A.M. Feasibility analysis of grid-connected and islanded operation of a solar PV microgrid system: A case study of Iraq. *Energy* **2020**, *191*, 116591.
15. Adefarati, T.; Bansal, R.C. The Impacts of PV-Wind-Diesel-Electric Storage Hybrid System on the Reliability of a Power System. *Energy Procedia* **2017**, *105*, 616–621. [CrossRef]
16. Maleki, A.; Rosen, M.A.; Pourfayaz, F. Optimal operation of a grid-connected hybrid renewable energy system for residential applications. *Sustainability* **2017**, *9*, 1314. [CrossRef]
17. Miceli, R. Energy management and smart grids. *Energies* **2013**, *6*, 2262–2290. [CrossRef]
18. Oyekale, J.; Petrollese, M.; Tola, V.; Cau, G. Impacts of Renewable Energy Resources on Effectiveness of Grid-Integrated Systems: Succinct Review of Current Challenges and Potential Solution Strategies. *Energies* **2020**, *13*, 4856. [CrossRef]
19. Javaid, N.; Ullah, I.; Akbar, M.; Iqbal, Z.; Khan, F.A.; Alrajeh, N.; Alabed, M.S. An intelligent load management system with renewable energy integration for smart homes. *IEEE Access* **2017**, *5*, 13587–13600. [CrossRef]
20. Armin, R.A.; Sumper, A.; Davarpanah, A. Energy sustainability analysis based on SDGs for developing countries. *Energy Sources Part A Recovery Util. Environ. Eff.* **2020**, *42*, 1041–1056. [CrossRef]
21. Chakir, A.; Tabaa, M.; Moutaouakkil, F.; Medromi, H.; Alami, K. Smart multi-level energy management algorithm for grid-connected hybrid renewable energy systems in a micro-grid context. *Energy* **2020**, *12*, 055301.
22. Armin, R.A.; Sumper, A.; Davarpanah, A. Development of sustainable energy indexes by the utilization of new indicators: A comparative study. *Energy Rep.* **2019**, *5*, 375–383. [CrossRef]
23. Mansour, A.; Gabash, A.; Li, P. Optimal Operation Strategy of a Hybrid PV-Battery System under Grid Scheduled Blackouts. In Proceedings of the2017 IEEE International Conference on Environment and Electrical Engineering and 2017 IEEE Industrial and Commercial Power Systems Europe (EEEIC/I&CPS Europe), Milan, Italy, 6–9 June 2017.
24. Le problème de l'industrialisation du Cameroun. Available online: http://georepere.e-monsite.com/medias/files/chap.26.industrialisation.dun.cameroun.pdf (accessed on 7 April 2021).
25. Photovoltaic Geographical Information System. Available online: https://re.jrc.ec.europa.eu/pvg_tools/fr/#PVP (accessed on 7 February 2021).
26. PopulationData.net. Available online: https://www.populationdata.net/pays/cameroun/ (accessed on 25 March 2021).
27. Yahia, B.; Arab, A.H.; Azoui, B. Optimal sizing of photovoltaic pumping system with water tank storage using LPSP concept. *Sol. Energy* **2011**, *85*, 288–294.
28. Fadaee, M.; Radzi, M.A.M. Multi-objective optimization of a stand-alone hybrid renewable energy system by using evolutionary algorithms: A review. *Renew. Sustain. Energy Rev.* **2012**, *16*, 3364–3369. [CrossRef]
29. Ma, T.; Yang, H.; Lu, L.; Peng, J. Pumped storage-based standalone photovoltaic power generation system: Modeling and techno-economic optimization. *Appl. Energy* **2015**, *137*, 649–659. [CrossRef]
30. Mahmoudimehr, J.; Shabani, M. Optimal design of hybrid photovoltaic-hydroelectric standalone energy system for north and south of Iran. *Renew. Energy* **2018**, *115*, 238–251. [CrossRef]
31. Yang, H.; Zhou, W.; Lu, L.; Fang, Z. Optimal sizing method for stand-alone hybrid solar–wind system with LPSP technology by using genetic algorithm. *Sol. Energy* **2008**, *82*, 354–367. [CrossRef]
32. Koutroulis, E.; Kolokotsa, D.; Potirakis, A.; Kalaitzakis, K. Methodology for optimal sizing of stand-alone photovoltaic/wind-generator systems using genetic algorithms. *Sol. Energy* **2006**, *80*, 1072–1088. [CrossRef]
33. Abdelkader, A.; Rabeh, A.; Ali, D.M.; Mohamed, J. Multi-objective genetic algorithm based sizing optimization of a stand-alone Wind/PV power supply system with enhanced battery/supercapacitor hybrid energy storage. *Energy* **2018**, *163*, 351–363. [CrossRef]
34. Mahesh, A.; Sandhu, K.S. A genetic algorithm based improved optimal sizing strategy for solar-wind-battery hybrid system using energy filter algorithm. *Front. Energy* **2020**, *14*, 139–151. [CrossRef]
35. Chandel, S.S.; Nagaraju, N.M.; Chandel, R. Review of solar photovoltaic water pumping system technology for irrigation and community drinking water supplies. *Renew. Sustain. Energy Rev.* **2015**, *49*, 1084–1099. [CrossRef]
36. Niknam, P.H.; Talluri, L.; Fiaschi, D.; Manfrida, G. Improved Solubility Model for Pure Gas and Binary Mixture of CO2-H2S in Water: A Geothermal Case Study with Total Reinjection. *Energies* **2020**, *13*, 2883. [CrossRef]
37. Yang, X.S. Firefly algorithm, stochastic test functions and design optimization. *Int. J. Bio-Inspired Comput.* **2010**, *2*, 78–84. [CrossRef]
38. Yang, X.S. *Nature-Inspired Optimization Algorithms*; Elsevier: Amsterdam, The Netherlands, 2014; ISBN 978-0-12-416743-8. [CrossRef]
39. Yang, X.S. *Firefly Algorithms for Multimodal Optimization, International Symposium on Stochastic Algorithms*; Springer: Berlin/Heidelberg, Germany, 2009; pp. 169–178.
40. Yang, X.S. Multiobjective firefly algorithm for continuous optimization. *Eng. Comput.* **2013**, *29*, 175–184. [CrossRef]